IEEE Access
Multidisciplinary | Rapid Review | Open Access Journal

Received April 25, 2022, accepted June 6, 2022, date of publication June 10, 2022, date of current version June 16, 2022.

Digital Object Identifier 10.1109/ACCESS.2022.3182032

Optimal Sizing of Different Energy Sources in an Isolated Hybrid Microgrid Using Turbulent Flow Water-Based Optimization Algorithm

MAHMOUD E. SALLAM[1], MAHMOUD A. ATTIA[1], ALMOATAZ Y. ABDELAZIZ[1], (Senior Member, IEEE), MARIAM A. SAMEH[2], AND AHMED H. YAKOUT[1]

[1]Faculty of Engineering, Ain Shams University, Cairo 11517, Egypt
[2]Department of Electrical Engineering, Future University in Egypt, Cairo 11835, Egypt

Corresponding author: Mariam A. Sameh (mariam.ahmed@fue.edu.eg)

ABSTRACT This paper proposes a relatively new optimization algorithm namely the Turbulent Flow Water-Based Optimization (TFWO) to find the optimal size of a hybrid isolated microgrid generation. Moreover, validation of the proposed algorithm is proved through a comprehensive comparison with three robust performance and fast convergence algorithms which are the Harris Hawks Optimization (HHO), Whale Optimization Algorithm (WOA) and Jellyfish Search Optimizer (JSO). Two topologies with different renewable sources were considered in studying which are based on the meteorological data of the Zafarana area, a site located on the eastern coast of Egypt. The study minimizes the annual system cost (ASC) and CO_2 emissions of the proposed hybrid system while considering the following constraints: Loss of Power Supply Probability (LPSP), Fraction Renewable (FR) and System Excess Energy Ratio (EER). Violation of constraints is penalized by including a penalty factor into the objective function that varies according to the amount of the violation. Moreover, a sensitivity study is presented at the end of the paper through Load variation, irradiance variation, wind speed variation, and diesel generator efficiency decreasing. Results show not only the robustness and the fast convergence of the TFWO algorithm but also its ability to minimize the annual system cost and emission costs to values better than the aforementioned optimization techniques.

INDEX TERMS EER, HHO, hybrid microgrid, optimal sizing, TFWO, hybrid renewable energy system, LPSP, penalty factor, renewable fraction, JSO, WOA.

I. INTRODUCTION

Most of world's energy production comes from fossil fuels, which have many environmental drawbacks such as greenhouse gas emissions and global warming [1], [2]. Moreover, the steady population growth and industrial developments lead to a continuous increase in energy demand, even in small cities and rural areas. A Diesel Generator (DG) can be used as a single source in these rural or isolated areas, however some problems still exist such as environmental drawbacks, fuel unavailability, fuel global price fluctuations, and lack of system controllability and flexibility [3]. Regarding the fact that fossil fuels are vulnerable to rapid depletion; Renewable energy systems are the best solution out there. But due to the stochastic intermittent nature of renewable energy sources (solar, wind), energy storage systems (ESS) are incorporated such as batteries [4]. Such a system with multiple distributed generators (Photovoltaic cells, Wind turbines, and DG), energy storage systems (ESS) and a cluster of loads is defined as a microgrid [5]–[7]. Microgrids can be either grid-connected or isolated (off-grid).

A proper planning and sizing of Hybrid Renewable Energy System (HRES) is essential for secure, reliable, and economic operation of microgrids [8]. This makes the optimal sizing of the HRES to be a multi-objective optimization problem which comprises a group of objectives such as minimizing the cost, CO_2 emission, excess energy while maximizing the system reliability [9]. Two optimization approaches were widely used to solve the sizing of the HRES problem, the classical (conventional) approach and meta-heuristic approach.

The associate editor coordinating the review of this manuscript and approving it for publication was Jamshid Aghaei.

Examples of classical optimization methods suggested in literature are Liner Programing, Dynamic Programing, and Iterative Optimization. Authors of [10] used the linear programming technique for minimizing the energy cost of system with different renewable energy sources. Also, authors of [11] implemented the linear programming approach in MATLAB software to find the optimal size considering the initial cost of a Wind/PV/micro-hydro hybrid system. Moreover, results were validated through a comparison with other numerical iterative methods. While, the dynamic programming method is presented in [12] to optimally manage the energy of an island microgrid comprising a PV system, DG and battery energy storage system considering the operation cost and emissions as objectives.

Furthermore, an iterative optimization method is used in [13] to optimize the size of a WIND system, photovoltaic (PV) system, and a hybrid WIND/PV system. Also, an enumeration-based iterative optimization algorithm used a single-objective optimal sizing approach for an islanded microgrid in [14]. This approach determines the optimal components size (N_{PV}, N_{Wind}, ...) for the hybrid microgrid, such that the total net present cost (TNPC) is minimized, while ensuring a low loss of power supply probability (LPSP). Moreover, a new iterative optimization, which is named iterative filter selection approach is introduced in [15] to find the optimal size of a PV/Wind/Battery hybrid renewable system while minimizing the total cost and maximizing the system reliability, then the results are compared to those obtained by Iterative-Pareto-fuzzy technique proving the superiority of the proposed approach.

Although the conventional optimization methods are used to find the optimal size of hybrid microgrids, they are not always appropriate for complex nonlinear systems. Therefore, the majority of recent researches consider Meta-heuristic optimization algorithms. Moreover, the Meta-heuristic optimization algorithms show better results when handling both single and multiple objective functions for optimally sizing a hybrid renewable microgrid. when a multiple objective function is proposed, multiple solutions can be found which are tradeoffs between these objectives and are called Pareto optimal solution. While in single objective function problems, the optimization technique is aiming to minimize or maximize a single objective function and a single optimal solution may be found.

With the rapid development of multi-objective evolutionary algorithms, many researches used them in finding the optimal size of HRES. In [16]–[18] a multi-objective genetic algorithm (GA) was used for sizing a HRES. The optimization aimed to minimize costs of the system (ASC, TNPC, and COE). While Authors of [19] used the non-dominated sorting genetic algorithm (NSGA-II) to optimize the HERS with the goal of minimizing the total system cost and Greenhouse gas emissions during the life cycle. Moreover, in [20], [21] NSGA-II was used with two objectives; the economic objective that minimizes the system total cost and the performance objective which maximizes system reliability. Another evolutionary algorithm; Particle Swarm Optimization (PSO) was used in [22], [23] to design a HRES. The Annual Capital Cost and the Cost of Energy (COE) were used as a single key objective for HRES sizing optimization. Furthermore, an improved PSO was introduced in [24] to find the optimal size of a hybrid PV-WIND-BATTERY system. The results of the system optimization were evaluated using an economic indicator; the levelized cost of electricity (LCE). Moreover, a hybrid GA-PSO method was proposed in [25] to find the optimal size of a hybrid microgrid using a single objective function.

In [26]–[29] cuckoo search algorithm (CSA), which is based on the brood reproductive strategy of cuckoo birds, was used to solve a single objective cost function. While, the reliability constraint Loss of Energy Probability (LOEP) and Loss of Power Supply Probability (LPSP) were used as a principle constraint. Also the social spider optimizer (SSO) was used in [30] to determine the optimal size of a hybrid renewable energy system (HRES), in which the cost of energy (COE) was proposed as a fitness function. while considering the LPSP as a constraint. While [31], [32] studies the effectiveness of the Grasshopper Optimization Algorithm (GOA) in the microgrid sizing problem against (PSO), (APSO), cuckoo search algorithm (CSA) and biogeography based optimization (BBO) algorithms.

In [33] a comparison and evaluation of the performance of various heuristic algorithms [(PSO), (GA), Salp Swarm algorithm (SSA) and Grey Wolf optimizer algorithm (GWO)] in sizing of a PV/WT/DG/battery hybrid systems were introduced based on a single objective function, the Total Annual Cost (TAC). The artificial bee colony (ABC) algorithm was implemented in [34], [35] to find the optimal configuration of a HRES, with the main decision variables selected to find the minimum costs (annual system cost ASC or Net Present Cost NPC). In [36] four optimization algorithms namely: BAT Algorithm (BA), Cuckoo Search Algorithm (CSA), Firefly Algorithm (FA), and Flower Pollination Algorithm (FP), were proposed to minimize the Life Cycle Cost (LCC) while considering (LPSP) as a constraint. Furthermore, authors of [37] minimize the Net Present Cost (NPC) using the Invasive Weed Optimization (IWO) and Particle Swarm Optimization (PSO). Also, the intelligent flower pollination algorithm (FPA) was implemented in MATLAB program in [38] to optimally size a microgrid considering the total net present cost (NPC) as the objective function and both the loss of energy expected (LOEE) and the loss of load expected (LOLE) as constraints.

While a Firefly Algorithm (FA) was adopted in [39], [40] to find the optimal sizing and rating of an island hybrid microgrid minimizing the costs NPC and operational cost of the suggested system. Also in [41], the dragonfly (DF) and firefly algorithm (FA) were used to find the minimum operating cost of micro grid both in grid connected mode and island mode. Dolphin echolocation algorithm (DEA) was introduced in [42] for sizing a photovoltaic system with the system's NPC correspondingly optimized. The DEA results

showed better elapsed time and net present value compared to Firefly Algorithm (FA) and Cuckoo search algorithm (CA). Moreover, recent algorithms named Chimp Optimization Algorithm (ChOA), Tunicate Swarm Algorithm (TSA), and Oppositional Runner Root Algorithm (ORRA) were used in [43]–[45], respectively to solve the sizing problem of a HERS using cost based objective function. In [46] novel optimization algorithms namely, Whale Optimization Algorithm (WOA), Water Cycle Algorithm (WCA), Moth-Flame Optimizer (MFO), and Hybrid particle swarm-gravitational search algorithm (PSOGSA) were applied for sizing hybrid microgrids.

The main idea of this paper is to propose the state of art of HERS optimization by applying recent optimization algorithms which guarantee the highest reliability, least environmental impact, and economical costs (capital and operational). The main contributions of this paper can be summarized as follows:

1. A recent optimization algorithm called Turbulent Flow Water-Based Optimization (TFWO) is proposed for the first time to find the optimal size of an isolated PV/WIND/DG/Battery hybrid microgrids.
2. A comprehensive comparison between the results of the proposed TFWO algorithm and three recent optimizations techniques the Harris Hawks Optimization (HHO), Whale Optimization Algorithm (WOA) and Jellyfish Search Optimizer (JSO) is introduced and evaluated.
3. The optimal sizing problem minimizes the annual system cost (ASC) of the proposed hybrid microgrid and CO2 system emissions while considering the following three constraints: Loss of Power Supply Probability (LPSP), Fraction Renewable (FR) and Excess Energy Ratio (EER).
4. LPSP, FR, and EER constraints are incorporated into the objective function as a penalty factors to ensure all solutions are within the constraint limits.
5. A case study based on meteorological data of Zafarana site located on eastern costal of Egypt has been presented, with a comprehensive sensitivity analysis.

This paper is organized as follows: section I is the introduction and literature review. Section II introduces mathematical model of the microgrid system components. The problem formulation, optimization objectives and constraints are presented in section III. The proposed optimization algorithms are discussed in Section IV. Moreover, section V introduces the two different topology case studies. Optimization results, comparisons and discussions are summarized in Section VI. Sensitivity analysis for both Microgrid topologies are introduced in section VII. Finally, Section VIII is the conclusion.

II. MATHEMATICAL MODEL OF THE MICROGRID COMPONENTS

The Proposed micro-grid is composed of solar Photovoltaic (PV), wind turbines (WT), diesel generator (DG), BESS (batteries) and AC loads as shown in FIGURE 1. The DG and loads are connected to the AC bus, while the PV, WT, and the BESS are connected to the DC bus. An inverter is connected between the DC and AC bus. The equations describing the performance of each source are presented in the following subsections.

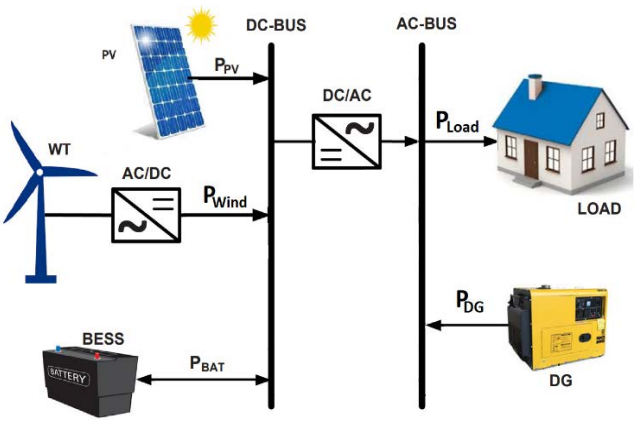

FIGURE 1. The configuration of proposed Microgrid.

A. PHOTOVOLTAIC (PV) SYSTEM

The energy supplied by the proposed PV system can be calculated as a function of solar irradiance and ambient temperature using equation (1) [3], [36]–[39], [47], [48]:

$$P_{PV}(t) = N_{PV}\eta_{PV}P_{PV_{rated}}\frac{G(t)}{G_{norm}}\left(1-\beta_T\left(T_C(t)-T_{norm}\right)\right) \quad (1)$$

where N_{PV} is the number PV panels in the microgrid, $P_{PV_{rated}}$ is the rated power of the PV panel at standard operating conditions ($G_{norm} = 1000W/m^2$ and $T_{norm} = 25°C$), η_{PV} is conversion efficiency of the PV panels, G (t) is the solar radiation intensity at any time t, G_{norm} is the intensity of solar radiation under standard conditions, β_T is the temperature coefficient of power of the selected PV panel, T_{norm} is the cell temperature under standard conditions of operation, and T_C (t) is the cell temperature which can be mathematically formulated as in equation (2) [3], [46]–[48]:

$$Tc(t) = T_{amb}(t) + \frac{G(t)}{800}\times(T_{noc}-20) \quad (2)$$

where T_{noc} is the normal cell operating temperature, and T_{amb} (t) is the ambient temperature in °C. Eq. (2) can be simplified as shown in equation (3) [23], [31], [33]:

$$Tc(t) = T_{amb}(t) + 0.0254\times G(t) \quad (3)$$

B. WIND TURBINE SYSTEM

Based on the basics of aerodynamics and wind energy, the power generated from the wind turbine at a certain wind speed can be mathematically expressed as the following

equation [46], [49], [50]:

$$P_{wind}(t) = \begin{cases} 0, & v(t) < v_{cut\_in}, v(t) > v_{cut\_off} \\ N_{wt}\eta_{wt}P_{wt_{rated}}\dfrac{v^2(t) - v^2_{cut\_in}}{v^2_{rated} - v^2_{cut\_in}}, & v_{cut\_in} < v(t) < v_{rated} \\ N_{wt}\eta_{wt}P_{wt_{rated}}, & v_{rated} < v(t) < v_{cut\_off} \end{cases} \quad (4)$$

where $P_{wt_{rated}}$ is the wind turbine rated power, N_{wt} is the number of wind turbines, η_{wt} is the efficiency of the wind system, $v_{cut_in}$is the wind speed at which the turbine starts to operate. While, v_{cut_off} is the wind speed after which the wind turbine must be shut down for safety reasons. Finally, v_{rated} is the wind speed at rated power. Taking into considerations that wind speed varies with height, so wind speed at various elevation can be calculated using the expression in equation (5) [46], [50]:

$$v = v_{ref}\left(\frac{h}{h_{ref}}\right)^{\alpha} \quad (5)$$

where v_{ref} is wind speed at reference height h_{ref} and α is the friction coefficient that usually has a value between 0.14 and 0.25 [1], [38], [39], [46].

C. DIESEL GENERATOR (DG)

The DG is employed in the isolated micro-grid as a secondary power supply in case of battery depletion and/or peak load. For acceptable efficiency level, lightly loaded or unloaded operation of DG should be avoided [46], [51]. Moreover, the optimum operating range for the individual DG is taken to be above 30% to 100% of its rated power [11]. The hourly fuel consumption of DG can be calculated using the formula in equation (6) [30], [31], [46]:

$$F(t) = 0.246 \times P_{DG}(t) + 0.08415 \times P_{DG\_rated} \quad (6)$$

where $P_{DG}(t)$ is the DG power at instant t, and P_{DG_rated} is the rated power of DG.

D. BATTERY ENERGY STORAGE SYSTEM (BESS)

The battery bank, which is a lead-acid type in this study, is used to store surplus generated energy when production exceeds consumption and to keep a constant flow of power to the desired load during shortage periods of renewable sources. One of the important parameters defining the residual capacity state of the battery bank is the state of charge (SOC). The state of charge (SOC) can be calculated as in equation (7):

$$SOC(t) = \frac{C(t)}{C_{total}} \quad (7)$$

where, $C(t)$ is the BESS capacity at each instant and C_{total} is the total capacity. Moreover, at the moment t, the stage of charge $SOC(t)$ is related to the previous stage of charge $SOC(t-1)$ according to equation (8) and (9) [31], [37], [51].

– In case of charging:

$$SOC(t) = SOC(t-1) \times (1-\sigma) + \eta_{\text{batt}}\left[P_{pv}(t) + P_{wind}(t) - \frac{P_{load}(t)}{\eta_{\text{inv}}}\right] \times \Delta t \quad (8)$$

– In case of discharging:

$$SOC(t) = SOC(t-1) \times (1-\sigma) + \eta_{\text{batt}}\left[\frac{P_{load}(t)}{\eta_{\text{inv}}} - P_{pv}(t) - P_{wind}(t)\right] \times \Delta t \quad (9)$$

where σ, η_{batt} and η_{inv} are self-discharge rate, battery efficiency and inverter efficiency respectively.

III. CONTROL STRATEGY

In this section control strategy, objective function and the constraints will be presented in details to achieve economic supply of energy.

A. CONTROL STRATEGY OF MICROGRID OPERATION

Due to the unpredictable nature of renewable resources, suitable control strategy should be considered to supply the load at different weather conditions and different times of the day. The control strategy considered in our study can be summarized as:

1. When the renewable energy is equal or larger than the load the DG will not operate and the power difference can be presented as in equation (10):

$$\Delta P = (P_{\text{pv}}(t) + P_{\text{wind}}(t)) - P_{\text{load}}(t)/\eta_{\text{inv}} \quad (10)$$

   Moreover, based on the SOC of the battery we have three situations:
   – If ΔP equals zero the battery will neither charged nor discharged.
   – If ΔP is than zero and the battery is not fully charged, the surplus energy will charge the battery.
   – If $\Delta P$is greater than zero and the battery is fully charged the system will suffer from excess energy.
2. On the other hand if the renewable energy is less than the load, then the batteries will discharge and recompense the power difference (ΔP) as in equation (11).

$$E_{\text{batt}}(t) = |\Delta p| \times \Delta t \quad (11)$$

3. But if the batteries cannot compensate for the whole power difference, then the DG will operate one of the following states:
   – If the shortage of the energy is less than the minimum DG power[P_{DGmin}], then the DG will compensate the whole power difference and charge the batteries as in equation (12).

$$\frac{E_{DGmin}(t)}{\eta_{\text{inv}}} = |\Delta p| \times \Delta t + E_{\text{batt}}(t) \quad (12)$$

– If the shortage of the energy is more than the minimum DG power [P_{DGmin}], then the DG and the batteries will act together to compensate the whole power difference according to equations (13),(14) of batteries as follows:

$$|\Delta p| \times \Delta t = E_{batt}(t) + \frac{E_{DGmin}(t)}{\eta_{inv}}, \text{ where}$$
$$E_{batt}(t) + \frac{E_{DGmin}(t)}{\eta_{inv}} \geq |\Delta p| \times \Delta t \quad (13)$$

$$|\Delta p| \times \Delta t = E_{batt}(t) + \frac{E_{DG}(t)}{\eta_{inv}}, \text{ where}$$
$$E_{batt}(t) + \frac{E_{DGmin}(t)}{\eta_{inv}} < |\Delta p| \times \Delta t \quad (14)$$

Moreover, FIGURE 2 presents the flow chart of the system under different renewable energy operation modes.

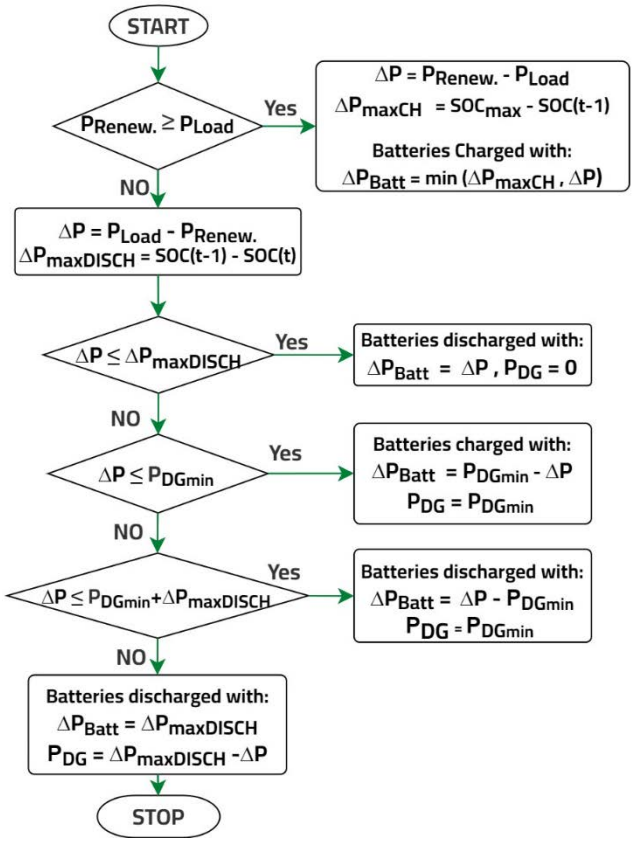

FIGURE 2. Flowchart of the proposed control strategy of Microgrid.

B. OBJECTIVE FUNCTION

The objective function is chosen to minimize the annual cost of system (ACS) considering the CO2 emission and the fuel cost. It comprises the initial investment cost and the operating payments throughout the life time of installation. For this study, the lifetime of components is taken to be 20 years, while the BESS life time is taken to be 10 years.

The annual system cost (ASC) is considered as shown in equation (15) [46], [47]:

$$ASC = ACC + ARC + AOM + AFC + AEC \quad (15)$$

where ACC is the annual capital cost, ARC is the annual replacement cost, (AOM) is the annual operation and maintenance cost, (AFC) is the annual fuel cost, and (AEC) is the annual emission cost. And each of this costs will be presented in detail.

1. Annual capital cost (ACC) can be calculated by equation (16) [46]:

$$ACC = ACC_{PV} + ACC_{wind} + ACC_{DG} + ACC_{Batt} + ACC_{Invert.} \quad (16)$$

where ACC_{PV}, ACC_{wind}, ACC_{DG}, ACC_{Batt}, and $ACC_{Invert.}$ are the installation annual capital cost of the PV system, wind system, DG, battery bank, and inverter, respectively. The annual capital cost for each component can be calculated using equation (17), (18) [34], [37], [46], [47].

$$ACC = CRF(i_r, y) \times C_{capital} \quad (17)$$

$$\text{in which,} \quad CRF(i_r, y) = \frac{i_r \times (1+i_r)^y}{(1+i_r)^y - 1} \quad (18)$$

where $C_{capital}$ is the capital cost, CRF is the capital recovery factor which is a ratio used to calculate the present value of an annuity (a series of equal annual cash flows) [47], y is the project lifetime in years and i_r is the real interest rate (or called real discount rate).

2. The ARC annual replacement cost for each component is the annual preset value of replacement cost of the hybrid system components within the system lifetime and can be calculated using equations (19),(20).

$$ARC = SFF(i_r, y_{rep}) \times C_{replacement} \quad (19)$$

$$\text{in which,} \quad SFF(i_r, y_{rep}) = \frac{i_r}{(1+i_r)^{y_{rep}} - 1} \quad (20)$$

where $C_{replacement}$ is the component replacement cost, SFF is the sink fund factor which is a ratio used to calculate the future value of a series of equal annual cash flows, y_{rep} is the component lifetime in years and i_r is the real interest rate.

3. The AOM annual operation and maintenance cost can be calculated as a percentage of the capital cost of the component divided by the project lifetime y. This value is specific to each component model.
4. The AFC annual fuel cost of DG can be calculated as in equation (21) [12], [47].

$$AFC = C_F \sum_{t=1}^{8760} F(t) \quad (21)$$

where C_F is the fuel cost per liters and $F(t)$ is the hourly fuel consumption of DG presented by equation (6).

5. The AEC annual CO_2 emission cost is calculated as in equation (22) [12], [47].

$$AEC = \sum_{t=1}^{8760} \frac{E_f E_{fc} P_{DG}(t)}{1000} \tag{22}$$

where E_f is the emission factor of DG (7.09×10^{-4} tons CO2/kWh [52]), E_{fc} is the emission cost factor and $P_{DG}(t)$ is the diesel power at instant (t).

C. OPTIMIZATION CONSTRAINTS

1) THE OPERATION CONSTRAINTS

The number of PV panels (N_{PV}), number of wind turbines (N_{WIND}), BESS capacity (C_{Batt} in Watt), BESS SOC, and DG rated power (P_{R_DG} in Watt) are constrained by minimum and maximum values as shown in equations (23-27). Furthermore, the balance between the generation and load demand power is considered as another operation constraint, as in equation (28) [12], [47].

$$N_{PV} = integer, \quad 0 < N_{PV} \leq N_{PV\_MAX} \tag{23}$$

$$N_{Wind} = integer, \quad 0 < N_{Wind} \leq N_{Wind\_MAX} \tag{24}$$

$$C_{Batt}\ in\ watt, \quad 0 < C_{Batt} \leq C_{Batt\_MAX} \tag{25}$$

$$SOC_{min.} \leq SOC(t) \leq SOC_{max.} \tag{26}$$

$$P_{DG\_min.} \leq P_{DG}(t) \leq P_{Load\_peak} \tag{27}$$

$$P_{load}(t) = P_{pv}(t) + P_{wind}(t) + P_{batt}(t) + P_{DG}(t) \tag{28}$$

2) LOSS OF POWER SUPPLY PROBABILITY (LPSP)

Another constraint considered in our study is the LPSP defined as the probability of insufficient operation of the power supply when the isolated hybrid renewable system fails to satisfy the demand for energy [46]. The value of LPSP is in range [0, 1] and can be obtained according to equations (29), (30) [25], [51]:

$$LPSP = \frac{\sum_{t=1}^{8760} LPS(t)}{\sum_{t=1}^{8760} P_{load}(t)} \tag{29}$$

$$LPS(t) = P_{load}(t) - [P_{pv}(t) + P_{wind}(t) + P_{batt}(t) + P_{DG}(t)] \tag{30}$$

where $LPS(t)$ is the loss of power supply each hour and $P_{load}(t)$ is the load demand. The value of LPSP has to be less than a predefined reliability index β_L which is taken to be zero in our study to ensure a 100% reliable system [46], [49]. If the LPSP exceeds this value a penalty term in the objective function will force the optimization algorithm to consider this solution infeasible.

3) EXCESS ENERGY RATIO (EER)

The excess energy ratio can be calculated by dividing the excess renewable energy by the total energy production as in equations (31-32)

$$EER = \frac{\sum E_{excess}}{\sum E_{pv} + \sum E_{wind} + \sum E_{DG}} \tag{31}$$

$$E_{excess}(t) = [P_{pv}(t) + P_{wind}(t) - P_{batt}(t) - P_{load}(t)] \times \Delta t \tag{32}$$

In our study the excess energy ratio is forced to be zero by applying a penalty term in the objective function that will force the optimization algorithm to consider any solution with an EER value other than zero to be infeasible.

4) RENEWABLE FRACTION (RF)

RF is calculated to indicate the amount of renewable power generated to DG power generated; the objective is to minimize diesel output which in case will minimize operation cost and CO2 emissions. RF can be calculated using equation (33) [22], [51], [59]:

$$RF = \left(1 - \frac{\sum P_{DG}}{\sum (P_{pv} + P_{wind})}\right) \times 100 \tag{33}$$

where $\sum (P_{pv} + P_{wind})$ represents the annual total generated renewable power and $\sum P_{DG}$ is the annual total diesel generator power. The value of RF has to be greater than a predefined value which is taken to be 70% in our study. If the RF violates this constraint, a penalty term in the objective function will force the optimization algorithm to consider this solution infeasible.

IV. TURBULENT FLOW OF WATER-BASED OPTIMIZATION (TFWO)

TFWO is a metaheuristic algorithm inspired from whirlpools created in water turbulences where the water forms helical paths due to the force of gravity leading to the formation of a whirlpool. The center of whirlpool acts as a sucking hole, and draws the objects around it by effect of centripetal force. The TFWO main steps are presented in FIGURE 3 and can be summarized as follows [57]:

- The initialization phase: The initial search agent population (X_O) is divided equally into N_{Wh} whirlpool groups. Then the search agent with the best fitness function in each group is identified as the central whirlpool.
- Phase ONE: In this phase the central whirlpool in each group is trying to unify the position of all the search agents to its position Z_j. Therefore, any i^{th} search agent make an angle δ_i with the central whirlpool, this angle will be changed to simulate plunging into the central whirlpool. The new value of this angle δ_i^{new} can be calculated according to equation (34).

$$\delta_i^{new} = \delta_i + \pi * rand_1 * rand_2 \tag{34}$$

where $rand_1$ and $rand_2$ are random numbers between [0,1] and δ_i represents the search agent angle with its whirlpool group center.

Moreover, whirlpools in the other groups can also change the position of the search agents in whirlpool group j. Therefore, the search agent position under the influence of these effects will be updated to a new position X_i^{new} according to equation (35).

$$X_i^{new} = Z_j - \Delta X_i \tag{35}$$

where Z_j is the position of whirlpool group j center and ΔX_i is the search agent position displacement which is calculated by equation (36).

$$\begin{aligned}\Delta X_i = &(\cos\left(\delta_i^{new}\right) * rand\ (1, D) * \left(Z_f - X_i\right) \\ &- \sin\left(\delta_i^{new}\right) * rand\ (1, D) * (Z_w - X_i)) \\ &* \left(1 + \left|\cos\left(\delta_i^{new}\right) - \sin\left(\delta_i^{new}\right)\right|\right)\end{aligned} \tag{36}$$

where δ_i^{new} is the new search agent angle with its whirlpool center, D represents the number of optimization variables, Z_w and Z_f are the most and least weighted distance (WD_t) for all search agents respectively and calculated by equation (37).

$$WD_t = f\ (Z_t) * \sqrt{\left|Z_t - \sum X_i\right|}) \tag{37}$$

where Z_t and $f(Z_t)$ is the position and fitness function of search agent t which is tested to find the most and least weighted distance (WD_t) to the current search agent i.

- Phase TWO (The exploration phase): The centrifugal force that counteracts the centripetal force of the moving objects tries to take them away from the whirlpool group center. If the centrifugal force (C*Fi*) can overcome the centripetal force, it will randomly move the search agent to a new position along one randomly chosen direction. The centrifugal force is calculated according to equation (38), then it is compared to a random number which has a uniform distribution in the range [0, 1]. If C*Fi* is greater than this random number, an optimization variable (p) is chosen randomly according to equation (39). The value of this selected optimization variable (p) is changed randomly to a new value, and then, the new position of the search agent in p-dimension can be calculated according to equation (40).

$$CF_i = \left(\left(\cos\left(\delta_i^{new}\right)\right)^2 * \left(\sin\left(\delta_i^{new}\right)\right)^2\right)^2 \tag{38}$$

$$p = round(1 + rand * (D - 1)) \tag{39}$$

$$x_{i,p} = x_p^{min} + rand * (x_p^{max} - x_p^{min}) \tag{40}$$

- Phase THREE: The interactions between the central whirlpools can also change their position i.e. the central whirlpool in each group is trying to unify the position of other central whirlpools to its position Z_j. Therefore, any j^{th} central whirlpool have an angle δ_j, this angle will be changed to simulate plunging into other central whirlpools. The new value of this angle δ_j^{new} can be calculated according to equation (41).

$$\delta_j^{new} = \delta_j + \pi * rand_1 * rand_2 \tag{41}$$

where $rand_1$ and $rand_2$ are random numbers between [0,1] and δ_j represents the central whirlpool angle.
The central whirlpool j position will be updated to a new position Z_i^{new} according to equation (42).

$$Z_j^{new} = Z_f - \Delta Z_j \tag{42}$$

where ΔZ_i is the central whirlpool position displacement which is calculated by equation (43).

$$\begin{aligned}\Delta Z_j = &\ rand\ (1, D) * \left(Z_f - Z_j\right) \\ &* \left|\cos\left(\delta_j^{new}\right) + \sin\left(\delta_j^{new}\right)\right|\end{aligned} \tag{43}$$

where δ_j^{new} is the new central whirlpool angle, D represents the number of optimization variables, and Z_f is the minimum weighted distance (WD_t) to all whirlpools and is calculated using equation (44).

$$WD_t = f\ (Z_t) * \left|Z_t - \sum Z_j\right|) \tag{44}$$

where Z_t and $f(Z_t)$ is the position and fitness function of search agent t which is tested to find the minimum weighted distance (WD_t) to the current search agent i.

- Phase FOUR: The fitness function for all search agents and all Central whirlpools are recalculated based on the new positions. The search agents with the best fitness function among the whirlpool group is changed to be the group central whirlpool. A flow chart of TFWO algorithm is shown in FIGURE 3.

V. CASE STUDY

In order to demonstrate the validity and robustness of the proposed algorithm, results will be compared with other recent optimization techniques used in previous literature which are WAO, JSO, HHO. Our study considers two case studies with the same meteorological data (Zafrana, Egypt) and same power load profile, but with different generation sources. The first case Study considers an isolated micro-grid consisting of PV cells, Diesel generator (DG), and Battery Storage System (BESS), while the second study adds Wind turbines to the isolated micro-grid structure given in case study 1.

Zafrana (Lat. 29.115, Long. 32.658) is a coastal area in Egypt which is located on the western coast of the Red Sea, it is 200 km to the south east of Cairo city. Zafrana enjoys the brightness of the sun most days of the year and the average wind speed throughout the year is 8m/s. Moreover, two power load profiles are used in this study, one for summer days and one for winter days as shown in FIGURE 4 (a) and 4 (b) respectively. The hourly and monthly average solar irradiation is presented in FIGURE 5 [58]. While, FIGURE 6 presents the yearly wind speed average monthly wind speed for the selected area. Finally, the technical specifications and costs of the hybrid micro-grid system components are listed in TABLE 1.

VI. RESULTS AND DISCUSSION

The code of the proposed optimization techniques is implemented in MATLAB software package on PC processor

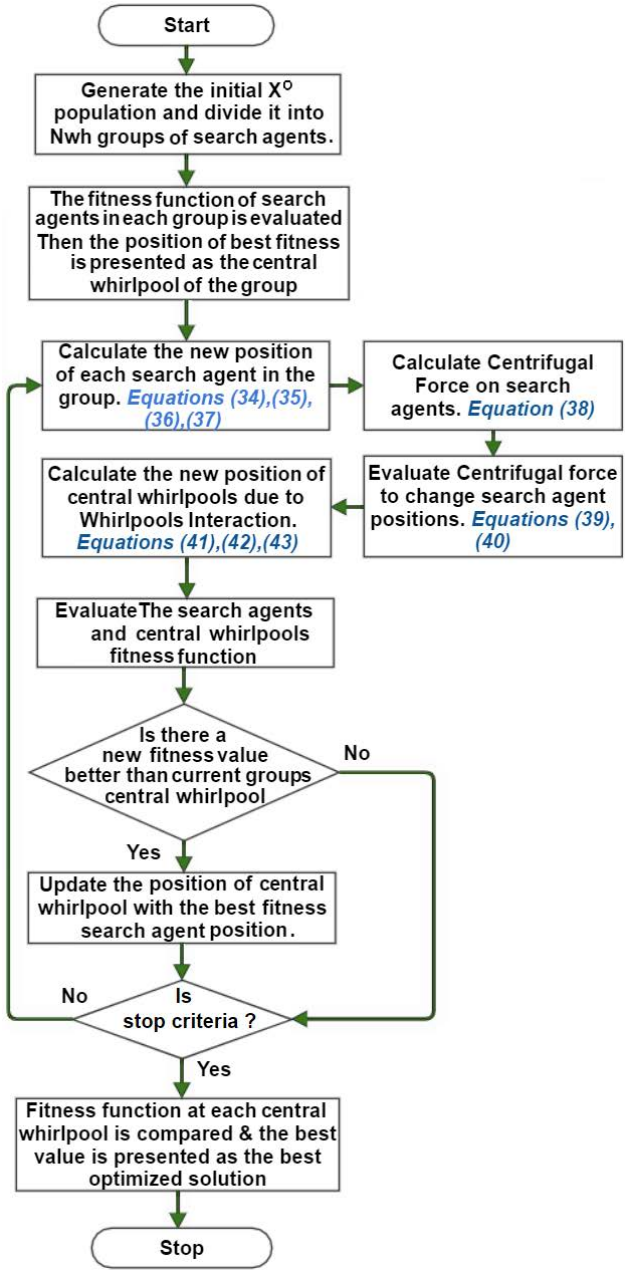

FIGURE 3. Flowchart of TFWO optimization algorithm.

Intel Core i5-1035G1 CPU@1.00GHz-1.19 GHz - 8.0 GB RAM. The optimization techniques are proposed with multiple objective function to minimize the ASC and CO_2 emissions based on the hourly available data. Furthermore, the Environmental constraint RF and the reliability constraints LPSP and EER are imposed on the objective function as a penalty term. The maximum number of iterations was set to 50 iterations and the optimization will be executed 20 times, for each run the best objective function (min. ASC) and the time of optimization per run will be stored. The average objective function, the standard deviation, and the average running time are calculated for the proposed TFWO and will be compared with HHO, JSO, and WOA techniques.

TABLE 1. Case technical specifications and costs of the hybrid micro-grid system components agents.

Component	Parameter	Value
PV	Capital Cost	280$
	Rated Power	260 watt
	Life time	20 years
Wind	Capital Cost	1500$
	Rated Power	1500watt
	Rated Speed	14 m/s
	Life Time	20 years
	Cut-in Wind speed	2.5 m/s
	Cut-out Wind speed	16 m/s
DG	Capital Cost	850$/K watt
	Fuel Cost	1 $/liters
	Emission function	0.34 kg/kWh
	DG Reliability	90%
	DG Life Time	20 years
Batteries	Capital Cost	244$/Wh
	Life Time	10 years
	Min. SOC%	20%
	Max. SOC%	90%
Project	Life Time	20 Years
	Interest rate	7%
	Inflation rate	5%

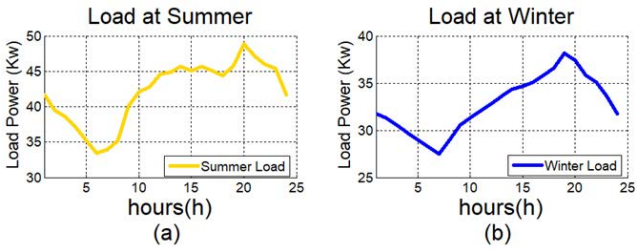

FIGURE 4. Hourly load demand (a) Summer day (b) Winter day.

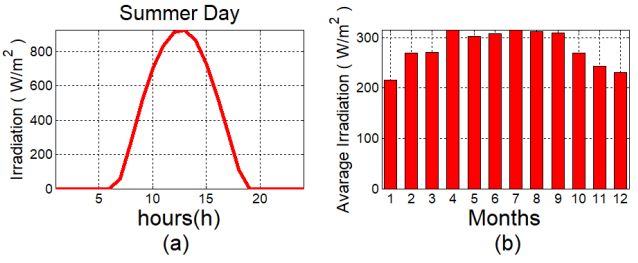

FIGURE 5. (a) Hourly solar irradiation data random day. (b) Average monthly irradiation data.

A. RESULTS OF CASE STUDY 1

In this case PV/DG/BESS hybrid microgrid is considered. TABLE 2 shows the optimization results of the presented algorithms (HHO, JSO, WOA, and TFWO) based on

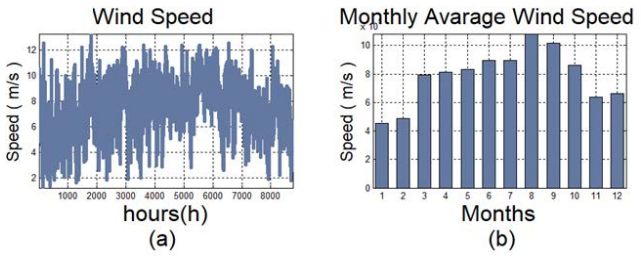

FIGURE 6. (a) Hourly Wind Speed in random day. (b) Average monthly Wind Speed (at 10 m).

TABLE 2. Case study 1 optimization results based on 50 search agents.

	HHO	JSO	WOA	TFWO
Min. ASC	83015.3$	82939.3$	82829.8$	**82789.1$**
Ava. ASC	85009.8$	83482.7$	84929.4$	**82843.0$**
Stand. Dev.	1274	3738.1	1465.2	**108.4**
Ava. time per run	5.97 Sec.	3.3 Sec.	2.65 Sec.	**2.45 Sec.**
N_{PV}	512	508	509	**510**
C_Batt	693350	675560	676795	**679502**
DG Rating	50.0 kw	49.937Kw	50.0 Kw	**50.0 Kw**
FR %	74.06 %	73.49 %	73.63 %	**73.77 %**
EER %	0.0 %	0.0 %	0.0 %	**0.0%**

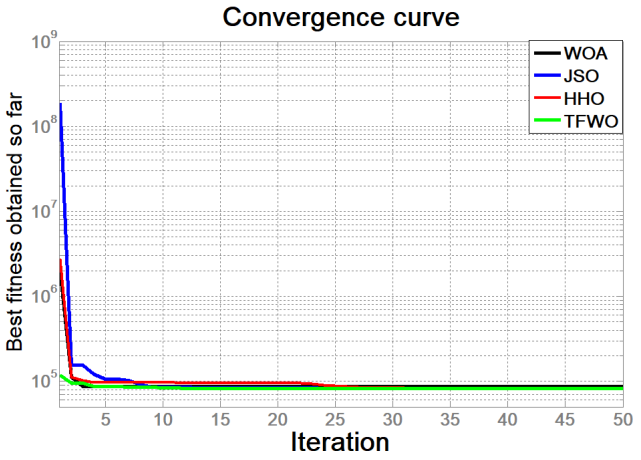

FIGURE 7. Convergence curves of optimization of proposed algorithms.

50 iteration and 50 search agents. Results show that minimum ASC (best fitness) is obtained by TFWO algorithm and is equal to 82789.1$ with the best standard deviation of 108.4$. Moreover, the convergence curves presented in FIGURE 7 confirm that TFWO has the fastest convergence among all optimization techniques, followed by the rest algorithms.

Moreover, results of size optimization of PV/DG/BESS hybrid microgrid system show that the optimum number of photovoltaic cells N_{PV} is 510 cells, the DG rated power P_{DG} is 50 kW, and Battery Capacity is 679.5 KWh. Furthermore, PV, DG, BESS, and load power balance for one summer week and one winter week are presented in FIGURE 8 (a) and 9 (a)

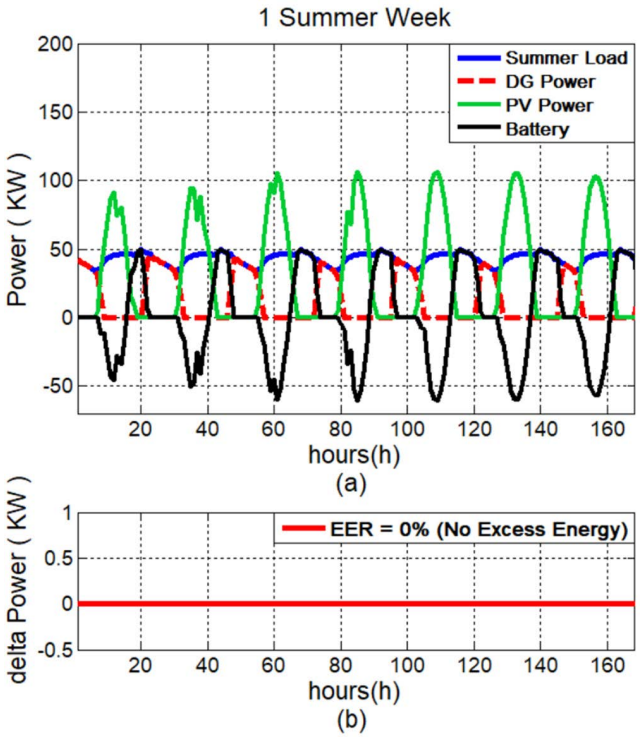

FIGURE 8. Variation of PV power, DG power and Battery Power along the summer day hours under optimal sizing results of Case Study 1, (a) 1 Summer Week Power, (b) Excess Energy for 7 summer days.

respectively and FIGURE 8 (b) and 9 (b) show that there is no excess energy in our case study results (i.e. EER% = 0).

B. RESULTS OF CASE STUDY 2

In case study 2 the wind power is incorporated into the microgrid system discussed in part A. Again each optimization technique is run for 20 times with 50 search agents and 50 iterations per run. Results show that minimum ASC (best fitness) is obtained by TFWO optimization it is equal to 79561.5$ which is better than ASC obtained in previous case.

TABLE 3 shows the optimal sizing results for the PV/WIND/DG/Battery hybrid isolated microgrid system using the following implemented algorithms (HHO, JSO, WOA, and TFWO).

The best obtained Annual cost of system (ASC) for PV/WIND/DG/BESS isolated micro-grid equals to 79561.5$, with photovoltaic cell number N_{PV} equals to 437 cells, wind turbine number N_{WIND} equals to 16 turbines, DG rated power (P_{DG}) equals to 46.205 kW, and Battery Capacity equals to 601.228 KWh. FIGURE 10 shows PV, WIND, DG, BESS, and load power flow balance for one summer week (168 hours) and another winter week (168 hours). As noticed for the entire year, no power deficiency is found and the energy from renewable resources (PV cells and Wind turbines) is totally used (EER=0%).

In TABLE 4 a detailed annual costs comparison between the DG only, Case Study 1, and Case Study 2 are introduced.

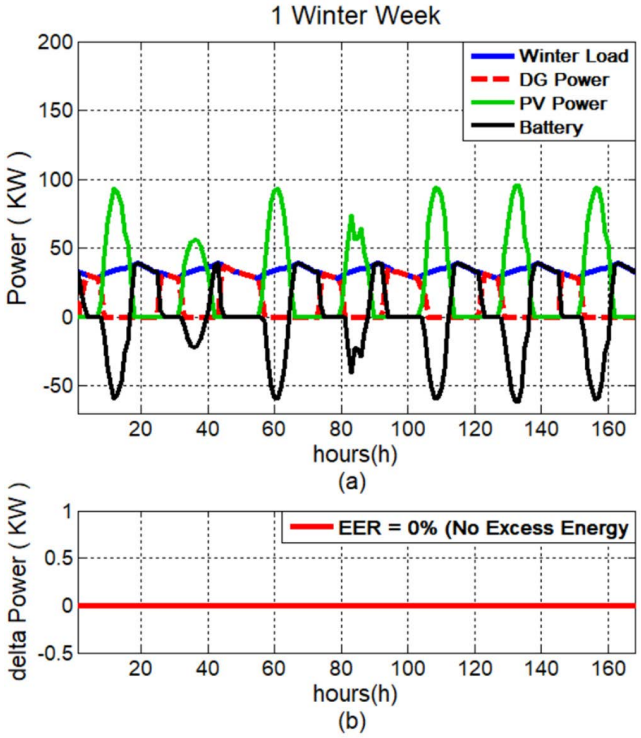

FIGURE 9. Variation of PV power, DG power and Battery Power along the winter day hours under optimal sizing results of Case Study One, (a) 1 Winter Week Power, (b) Excess Energy for 7 winter days.

TABLE 3. Case study 2 optimization results based on 50 search agents.

	HHO	JSO	WOA	TFWO
Min. ASC	80469.1$	79711.5$	79679.1$	**79561.5$**
Ava. ASC	87291.3$	81529.9$	82412.9$	**80143.8$**
Stand. Dev.	4984.9	1866	2204.9	**445.7**
Ava. time per run	32 Sec.	24.8 Sec.	15.7 Sec.	**11.5 Sec.**
N_{PV}	408	437	433	**437**
N_{WIND}	20	16	17	**16**
C_Batt	564601	604548	605270	**601228**
DG Rating	47.138Kw	46.283Kw	46.161Kw	**46.205Kw**
FR %	71.4 %	73.09 %	73.13 %	**73.09 %**
EER %	0.0 %	0.0 %	0.0 %	**0.0 %**

In case that only the DG was used to supply the load, the ASC equals to 135249.8$ and annual fuel cost equals to 119380.7$. In case study 1 (PV/DG/Battery) the ASC equals to 82789.1$ (reduced by 38.8% compared to DG only operation). In case study 2 (PV/WIND/DG/Battery) ASC equals to 79561.5$ with a bigger reduction equals to 41.2% compared to DG only operation. Also annual fuel cost reduced dramatically from 119380.7$ when DG only operation to 33949.7$ and 34741.8$ with case study one and case study two respectively.

VII. SENSITIVITY ANALYSIS

Here we study the effect of change of some input variables on the ASC. Because of intermittent nature of renewable energy sources, the irradiance and the wind speeds will be changed to test how the obtained optimal sizing method is robust and reliable. Moreover, the effect of DG efficiency deterioration and load change will be discussed as well.

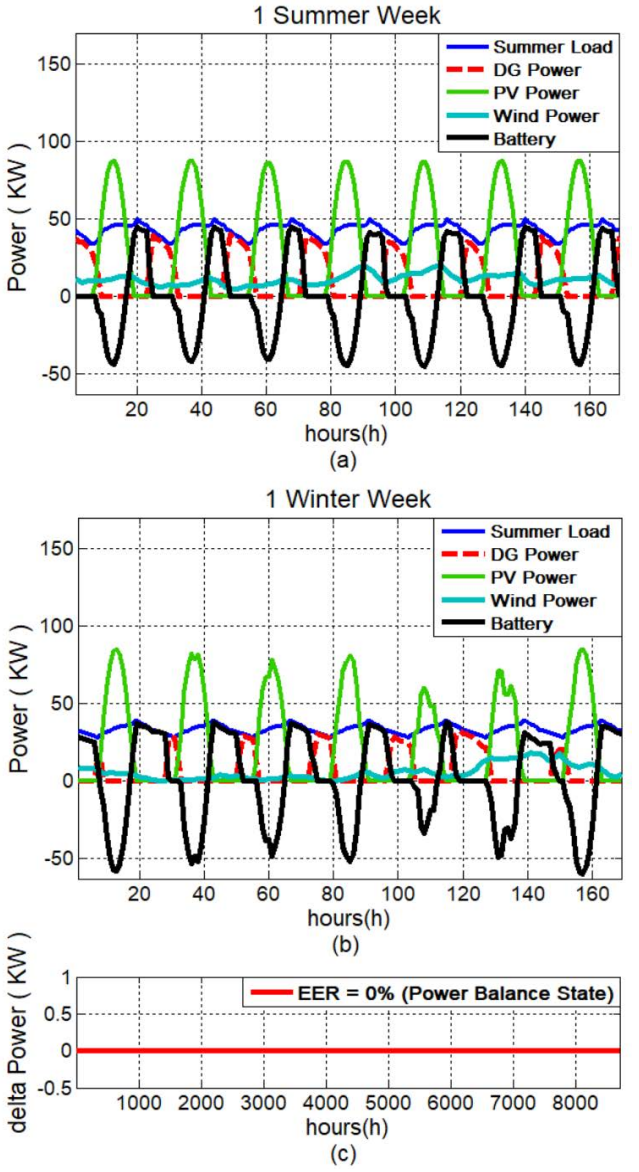

FIGURE 10. Variation of PV power, WIND Turbine, DG power and Batteries along the day hours under optimal sizing of Case Study Two, (a) Summer Day, (b) Winter Day, (c) Excess Energy for all year days.

A. SENSITIVITY ANALYSIS FOR CASE STUDY 1 (PV/DG/BATTERIES) ISOLATED MICRO-GRID

The effects of increasing the load on system costs, system reliability, and also system power balance are studied while keeping the photovoltaic cells N PV, DG rated power P DG, and Battery Capacity at their optimized values. TABLE 5 shows the PV/DG/Battery system costs and reliability while increasing load demand to 125% in 5% steps. As observed from the results that the Fuel cost, Emissions cost, and

TABLE 4. Case study 1, case study 2, and DG operating only results.

Annual Costs	Case Study 1	Case Study 2	DG only
ASC	82789.1 $	79561.5 $	135249.8$
Capital Cost	29317.1 $	27029.1 $	2575.3$
Fuel Cost	33949.7 $	34741.8 $	119380.7$
Emission Cost	3429.4 $	3518.8 $	13081.2$
O&M Cost	874.5 $	806.5 $	202.5 $
Replacement Cost Battery	15218.2 $	13465.2 $	0 $

TABLE 5. Case study 1 (PV/DG/Battery) sensitivity analysis on load demand (increase to 125% in steps of 5%).

Load	ASC	ΔASC%	Fuel Cost	Emission Cost	RF%	LPSP%
105%	89045$	7.5%	39554$	4082$	70.3%	0.00%
110%	94973$	14.7%	44831$	4733$	67.1%	0.02%
115%	100563$	21.5%	49790$	5364$	64.3%	0.17%
120%	106066$	28.1%	54700$	5957$	61.8%	0.55%
125%	110908$	34%	58982$	6516$	59.7%	1.11%

TABLE 6. Case study 1 (PV/DG/Battery) sensitivity analysis on PV Power (decrease irradiation by 20% in steps of 5%).

Irrad.	ASC	ΔASC%	Fuel Cost	Emission Cost	RF%	LPSP%
-5%	87225$	5.3%	37994$	3851$	70.6%	0.0%
-10%	91493$	10.5%	41805$	4280$	67.3%	0.0%
-15%	95854$	15.8%	45730$	4714$	63.9%	0.0%
-20%	100447$	21.3%	49883$	5156$	60.6%	0.0%

consequently the ASC increase when the load increases, which means that power deficiency is compensated mainly by DG operation to guarantee a high system reliability. For example, when the load increased to 105% from normal load values the increase in the ASC was about 7.5% while the LPSP value was kept at 0.0%, and when the load increased to 125% the LPSP increased to only 1.1%. Moreover, the RF% decreased from 73.77% to 59.69% when increasing the load from 100% to 125% due to DG operation.

The effect of the solar irradiation variation on the system costs can be studied by reducing the irradiation by 20% in 5% steps while fixing N_{PV}, P_{DG}, and Battery Capacity at their optimized values and not changing the load. In TABLE 6 the system costs and reliability when reducing the irradiation are shown. As observed the ASC increases proportional to the irradiation decrease while the LPSP value is fixed at 0% for all cases, i.e. when irradiation decreased by 5%, the ASC increased by about 5.3%, and so on. The fuel cost and emissions cost increase when the irradiation decreases, which means that the irradiation deficiency is compensated mainly by DG.

If the DG efficiency drops down, the DG rated power will drop down also while the fuel consumption increased.

TABLE 7. Case study 1 (PV/DG/Battery) sensitivity analysis of DG efficiency (efficiency drops down by 20% in steps of 5%).

DG Efficiency	ASC	ΔASC%	Fuel Cost	Emission Cost	RF%	LPSP%
-5%	84124$	1.6%	35105$	3609.8$	73.8%	0.00%
-10%	85589$	3.4%	36369$	3809.6$	73.8%	0.00%
-15%	87221$	5.3%	37780$	431.3$	73.8%	0.02%
-20%	88875$	7.3%	39209$	4255.8$	73.9%	0.19%

TABLE 8. Case study 2 (PV/WIND/DG/Battery) sensitivity analysis on load demand (increase to 125% in steps of 5%).

Load	ASC	ΔASC%	Fuel Cost	Emission Cost	RF%	LPSP%
105%	85660$	7.66%	40188$	4171$	69.6%	0.01%
110%	91555$	15.1%	45439$	4815$	66.5%	0.08%
115%	97157$	22.5%	49790$	5362$	63.7%	0.29%
120%	102479$	28.8%	55153$	6025$	61.3%	0.70%
125%	107459$	35.1%	59585$	6573$	59.3%	1.32%

TABLE 7 shows the (PV/DG/Battery) system costs and reliability when the DG efficiency drops down by 20% in 5% steps. The microgrid components size will be fixed at its optimized size. The results show that DG efficiency degradation effect on ASC is less significant compared to that of irradiation reduction i.e. the ASC increased by 1.6% when the efficiency decreased by 5%. Also the system reliability LPSP decreased to only 0.19% if the DG efficiency decreased by 20% from its nominal value. Moreover, it can be noticed that fuel cost and emissions cost increased with the reduction of DG efficiency.

B. SENSITIVITY ANALYSIS FOR CASE STUDY 2 (PV/WIND/DG/BATTERIES) ISOLATED MICRO-GRID

To study the effect of increasing the load on the optimized case study 2, only the load will be increased while fixing the photovoltaic cells N_{PV}, wind turbines N_{WIND}, DG rated power P_{DG}, and Battery Capacity at their optimized values. TABLE 8 shows the Case Study 2 (PV/WIND/DG/Batteries) system costs and reliability while increasing the load to 125% in 5% steps. It is noted from the results that the ASC increases when load increases, i.e. if load increases by 5% the ASC increases by 7.66% and reaches 35.1% when the load increased by 25%. The emission cost and fuel cost also increase with the increase of the load, which means that the DG operation is increased to compensate for the increased load which results in decrease the RF%. It was observed that effect of load increase on LPSP% was not large even with increasing the load to 125% where LPSP% reaches a value of 1.32%. This means that high reliability of the system is maintained while increasing the load.

Table 9 shows the Case Study 2 (PV/WIND/DG/Batteries) system costs and reliability when the irradiation decreased by 20% in 5% steps. We can notice that the power

TABLE 9. Case study 2 (PV/WIND/DG/Battery) sensitivity analysis on PV Power (decrease irradiation by 40% in steps of 10%).

Irrad.	ASC	ΔASC%	Fuel Cost	Emission Cost	RF%	LPSP%
-5%	83301$	4.7%	38118$	3881$	70.3%	0.0%
-10%	87060$	9.4%	41511$	4249$	67.5%	0.0%
-15%	90835$	14.2%	44913$	4621$	64.7%	0.0%
-20%	94751$	19.1%	48451$	4999$	61.8%	0.0%

TABLE 10. Case study 2 (PV/WIND/DG/Battery) sensitivity analysis on wind power (decrease Ava. wind speed by 20% in steps of 5%).

Wind Speed	ASC	ΔASC%	Fuel Cost	Emission Cost	RF%	LPSP%
-5%	81010$	1.8%	36041$	3668.7$	71.9%	0.00%
-10%	82332$	3.5%	37220$	3810.7$	70.7%	0.00%
-15%	83639$	5.1%	38393$	3944.8$	69.8%	0.00%
-20%	84849$	6.6%	39477$	4071.0$	68.9%	0.00%

TABLE 11. Case study 2 (PV/WIND/DG/Battery) sensitivity analysis of DG efficiency (efficiency drops down by 20% in steps of 5%).

DG Efficiency	ASC	ΔASC%	Fuel Cost	Emission Cost	RF%	LPSP%
-5%	80952$	1.7%	35947$	3704$	73.1%	0.00%
-10%	82468$	3.7%	37261$	3906$	73.1%	0.03%
-15%	84085$	5.7%	38658$	4126$	73.2%	0.1%
-20%	85753$	7.8%	40100$	4350$	73.3%	0.30%

deficiency is compensated again mainly by DG operation which is confirmed by significant increase in fuel cost and consequently the emissions cost. ASC increased by approximately the same percentage as the irradiation decreased, which is 5%. Also FR% decreased from 73.09% to 61.8% when irradiation decreased by 20%. LPSP is maintained at value of 0.0% when irradiation decreased by 20%.

Moreover, TABLE 10 shows the Case Study 2 (PV/WIND/DG/Batteries) system costs and reliability when the average wind speeds decreased by 20% in 5% steps. We can notice that the effect of the average wind speed decrease on ASC is not as severe as that of the irradiation decrease. The ASC increases by 1.8% if the average wind speed decreases by 5% and The increase of ASC due to 20% average wind speed decrease is 6.6%. The Wind power deficiency is compensated by both PV and DG, so the fuel cost and emission cost increasing ratio is not large like the previous case (irradiation decrease). Also, FR% decreased by a small rate with wind speed decreasing while LPSP is maintained at a 0.0% value even with max. wind speed reduction.

DG efficiency variation effects on the system costs can be studied on the optimized case study 2 by considering the normal load while decreasing the DG efficiency by 20% in 5% steps. TABLE 11 shows the Case Study 2 (PV/WIND/DG/Batteries) system costs and reliability when the DG efficiency drops down by 20% in 5% steps. The ASC, fuel cost and emission cost increase with DG efficiency decreasing, for example if DG efficiency drops down by 5% from its nominal efficiency the ASC increases by 1.7% and if DG efficiency drops down by 20% the ASC increases by 7.8%, and that is because the decrease of the DG efficiency is compensated by increasing the fuel consumption. The LPSP% dropped to 0.3% if the DG efficiency dropped to 20% while the RF% can be considered fixed (very small increase).

VIII. CONCLUSION

This paper presented an optimization model for sizing an isolated microgrid based on Energy control strategy which guarantees continuous power to the load at different climate conditions. The Loss of Power Supply Probability (LPSP), Renewable Fraction (RF), and Excess Energy Ratio (EER) are considered as a measure of the hybrid microgrid reliability. The optimization objective function is to minimize Annual system cost (ASC), Fuel cost, and Emission cost while maintaining the reliability constraints at the desired values by incorporating it as a penalty factor in the objective function. TWFO technique is implemented and its results are compared to HHO, JSO, and WOA optimization techniques.

The meteorological data for Zafrana, Egypt has been considered with two case studies; Case Study 1 which composites PV/DG/Battery systems, and Case Study 2 which composites PV/Wind/DG/Battery systems. Optimization results obtained by TFWO give the lowest ASC when compared with other optimization techniques. In case study 1 (PV/DG/Battery), the minimum ASC is 82789.1$ with $N_{PV} = 510$ cells, rated $P_{DG} = 50$ kW, Battery Capacity = 679.5 kWh, LPSP = 0.0%, EER = 0.0%, and finally RF = 73.77%. While, Case Study 2 (PV/WIND/ DG/Battery) the minimum ASC is 79561.5$ with $N_{PV} = 510$ cells, $N_{WIND} = 16$ turbines, DG rated power = 46.2 kW, Battery Capacity = 579.66 KWh, LPSP = 0.0%, EER = 0.0%, and finally RF = 73.09%.

Moreover, the sensitivity analysis has been carried out on both the two case studies to test the system durability and reliability with the Load variation, Irradiation variation, Wind variation, or DG efficiency dropping down. The results show that LPSP is maintained low for all studied cases, however, the ASC, Fuel Cost, and Emission Costs may slightly increase with load increase, solar irradiation decrease, or DG efficiency dropping down. Finally, optimal sizing of grid-connected microgrid taking into consideration the Egyptian electricity tariff and more types of renewable energy resources (such as biomass, hydro-electrical, and fuel cells) is recommended for future work.

REFERENCES

[1] M. Nurunnabi, N. K. Roy, E. Hossain, and H. R. Pota, "Size optimization and sensitivity analysis of hybrid wind/PV micro-grids- a case study for Bangladesh," *IEEE Access*, vol. 7, pp. 150120–150140, 2019, doi: 10.1109/ACCESS.2019.2945937.

[2] M. B. Shafik, G. I. Rashed, and H. Chen, "Optimizing energy savings and operation of active distribution networks utilizing hybrid energy resources and soft open points: Case study in Sohag, Egypt," *IEEE Access*, vol. 8, pp. 28704–28717, 2020, doi: 10.1109/ACCESS.2020.2966909.

[3] H. Chen, L. Gao, Z. Zhang, and H. Li, "Optimal energy management strategy for an islanded microgrid with hybrid energy storage," *J. Electr. Eng. Technol.*, vol. 16, no. 3, pp. 1313–1325, May 2021, doi: 10.1007/s42835-021-00683-y.

[4] F. Khlifi, H. Cherif, and J. Belhadj, "Sizing and multi-objective optimization of a multisource micro-grid with storage for an economic activity zone," in *Proc. Int. Conf. Adv. Syst. Emergent Technol. (IC_ASET)*, Mar. 2019, pp. 369–374, doi: 10.1109/ASET.2019.8871047.

[5] B. Lasseter, "Microgrids [distributed power generation]," in *Proc. IEEE Power Eng. Soc. Winter Meeting. Conf.*, Jan./Feb. 2001, pp. 146–149, doi: 10.1109/PESW.2001.917020.

[6] R. H. Lasseter, "MicroGrids," in *Proc. IEEE Power Eng. Soc. Winter Meeting Conf.*, vol. 1, 2002, pp. 305–308, doi: 10.1109/PESW.2002.985003.

[7] (2020). *About Microgrids—Microgrid Background*. Microgrid Institute. Accessed: May 22, 2021. [Online]. Available: http://www.microgridinstitute.org/microgrid-background.html

[8] A. A. Anderson and S. Suryanarayanan, "Review of energy management and planning of islanded microgrids," *CSEE J. Power Energy Syst.*, vol. 6, no. 2, pp. 329–343, Jun. 2020, doi: 10.17775/CSEEJPES.2019.01080.

[9] T. Tezer, R. Yaman, and G. Yaman, "Evaluation of approaches used for optimization of stand-alone hybrid renewable energy systems," *Renew. Sustain. Energy Rev.*, vol. 73, pp. 840–853, Jun. 2017, doi: 10.1016/j.rser.2017.01.118.

[10] R. Chedid and Y. Saliba, "Optimization and control of autonomous renewable energy systems," *Int. J. Energy Res.*, vol. 20, no. 7, pp. 609–624, 1996.

[11] F. A. Bhuiyan, A. O. Yazdani, and S. L. Primak, "Optimal sizing approach for islanded microgrids," *IET Renew. Power Generat.*, vol. 9, no. 2, pp. 166–175, 2014.

[12] N. A. Luu, Q.-T. Tran, and S. Bacha, "Optimal energy management for an island microgrid by using dynamic programming method," in *Proc. IEEE Eindhoven PowerTech*, Jun. 2015, pp. 1–6, doi: 10.1109/PTC.2015.7232678.

[13] W. D. Kellogg, M. H. Nehrir, G. Venkataramanan, and V. Gerez, "Generation unit sizing and cost analysis for stand-alone wind, photovoltaic, and hybrid wind/PV systems," *IEEE Trans. Energy Convers.*, vol. 13, no. 1, pp. 70–75, Mar. 1998, doi: 10.1109/60.658206.

[14] K. Kusakana, H. J. Vermaak, and B. P. Numbi, "Optimal sizing of a hybrid renewable energy plant using linear programming," in *Proc. IEEE Power Energy Soc. Conf. Expo. Afr., Intell. Grid Integr. Renew. Energy Resour. (PowerAfrica)*, Jul. 2012, pp. 1–5, doi: 10.1109/PowerAfrica.2012.6498608.

[15] S. Hussain, R. Al-Ammari, A. Iqbal, M. Jafar, and S. Padmanaban, "Optimisation of hybrid renewable energy system using iterative filter selection approach," *IET Renew. Power Gener.*, vol. 11, no. 11, pp. 1440–1445, Sep. 2017, doi: 10.1049/iet-rpg.2017.0014.

[16] B. O. Bilal, V. Sambou, P. A. Ndiaye, C. M. F. Kébé, and M. Ndongo, "Optimal design of a hybrid solar-wind-battery system using the minimization of the annualized cost system and the minimization of the loss of power supply probability (LPSP)," *Renew. Energy*, vol. 35, no. 10, pp. 2388–2390, 2010, doi: 10.1016/j.renene.2010.03.004.

[17] V. Suresh, M. Muralidhar, and R. Kiranmayi, "Modelling and optimization of an off-grid hybrid renewable energy system for electrification in a rural areas," *Energy Rep.*, vol. 6, pp. 594–604, Nov. 2020, doi: 10.1016/j.egyr.2020.01.013.

[18] S. K. Ramoji and B. R. Bibhuti, "Optimization of hybrid PV/wind energy system using genetic algorithm (GA)," *Int. J. Eng. Res. Appl.*, vol. 4, no. 1, pp. 29–37, 2014.

[19] Y. A. Katsigiannis, P. S. Georgilakis, and E. S. Karapidakis, "Multiobjective genetic algorithm solution to the optimum economic and environmental performance problem of small autonomous hybrid power systems with renewables," *IET Renew. Power. Gener.*, vol. 4, no. 5, pp. 404–419, Sep. 2010.

[20] A. Kamjoo, A. Maheri, A. M. Dizqah, and G. A. Putrus, "Multi-objective design under uncertainties of hybrid renewable energy system using NSGA-II and chance constrained programming," *Int. J. Elect. Power Energy Syst.*, vol. 74, pp. 187–194, Jan. 2016, doi: 10.1016/j.ijepes.2015.07.007.

[21] H. Bilil, G. Aniba, and M. Maaroufi, "Multiobjective optimization of renewable energy penetration rate in power systems," *Energy Proc.*, vol. 50, pp. 368–375, Jun. 2014, doi: 10.1016/j.egypro.2014.06.044.

[22] S. Upadhyay and M. P. Sharma, "Development of hybrid energy system with cycle charging strategy using particle swarm optimization for a remote area in India," *Renew. Energy*, vol. 77, pp. 586–598, May 2015, doi: 10.1016/j.renene.2014.12.051.

[23] P. Wang, W. Wang, and D. Xu, "Optimal sizing of distributed generations in DC microgrids with comprehensive consideration of system operation modes and operation targets," *IEEE Access*, vol. 6, pp. 31129–31140, 2018.

[24] C. Shang, D. Srinivasan, and T. Reindl, "An improved particle swarm optimisation algorithm applied to battery sizing for stand-alone hybrid power systems," *Int. J. Electr. Power Energy Syst.*, vol. 74, pp. 104–117, Jan. 2016, doi: 10.1016/j.ijepes.2015.07.009.

[25] N. Ghorbani, A. Kasaeian, A. Toopshekan, L. Bahrami, and A. Maghami, "Optimizing a hybrid wind-PV-battery system using GA-PSO and MOPSO for reducing cost and increasing reliability," *Energy*, vol. 154, pp. 581–591, Jul. 2018.

[26] S. Khenfous, A. Kaabeche, Y. Bakelli, and K. M. Sba, "Optimal size of renewable hybrid system applying nature-inspired algorithms," in *Proc. Int. Conf. Wind Energy Appl. Algeria (ICWEAA)*, Algiers, Algeria, Nov. 2018, pp. 1–6.

[27] M. Bhoye, S. N. Purohit, I. N. Trivedi, M. H. Pandya, P. Jangir, and N. Jangir, "Energy management of renewable energy sources in a microgrid using cuckoo search algorithm," in *Proc. IEEE Students' Conf. Electr., Electron. Comput. Sci. (SCEECS)*, Mar. 2016, pp. 1–6, doi: 10.1109/SCEECS.2016.7509294.

[28] M. Modiri-Delsha, N. A. Rahim, S. S. Taheri, and S. J. Seyed-Shenava, "Optimal generation scheduling in microgrids by cuckoo search algorithm," in *Proc. 3rd IET Int. Conf. Clean Energy Technol. (CEAT)*, 2014, pp. 1–5, doi: 10.1049/cp.2014.1457.

[29] A. Mallikarjuna, J. C. Balachandra, M. Potli, and N. Venugopal, "Optimal sizing of wind/solar/hydro in an isolated power system using SMFFT based cuckoo search algorithm," in *Proc. IEEE 6th Int. Conf. Power Syst. (ICPS)*, Mar. 2016, pp. 1–6, doi: 10.1109/ICPES.2016.7584107.

[30] A. Fathy, K. Kaaniche, and T. M. Alanazi, "Recent approach based social spider optimizer for optimal sizing of hybrid PV/wind/battery/diesel integrated microgrid in aljouf region," *IEEE Access*, vol. 8, pp. 57630–57645, 2020.

[31] A. L. Bukar, C. W. Tan, and K. Y. Lau, "Optimal sizing of an autonomous photovoltaic/wind/battery/diesel generator microgrid using grasshopper optimization algorithm," *Sol. Energy*, vol. 188, pp. 685–696, Aug. 2019.

[32] A. A. Ghavifekr, A. Mohammadzadeh, and J. F. Ardashir, "Optimal placement and sizing of energy-related devices in microgrids using grasshopper optimization algorithm," in *Proc. 12th Power Electron., Drive Syst., Technol. Conf. (PEDSTC)*, Feb. 2021, pp. 1–4, doi: 10.1109/PEDSTC52094.2021.9405951.

[33] S. M. H. Baygi, A. Elahi, and A. Karsaz, "A novel framework for optimal sizing of hybrid stand-alone renewable energy system: A gray wolf optimizer," in *Proc. 3rd Conf. Swarm Intell. Evol. Comput. (CSIEC)*, Bam, Iran, Mar. 2018, pp. 1–5.

[34] S. Singh, M. Singh, and S. C. Kaushik, "Feasibility study of an islanded microgrid in rural area consisting of PV, wind, biomass and battery energy storage system," *Energy Convers. Manage.*, vol. 128, pp. 178–190, Nov. 2016.

[35] L. Ciabattoni, F. Ferracuti, G. Ippoliti, and S. Longhi, "Artificial bee colonies based optimal sizing of microgrid components: A profit maximization approach," in *Proc. IEEE Congr. Evol. Comput. (CEC)*, Jul. 2016, pp. 2036–2042, doi: 10.1109/CEC.2016.7744038.

[36] K. M. Sba, Y. Bakelli, A. Kaabeche, and S. Khenfous, "Sizing of a hybrid (photovoltaic/wind) pumping systembased on metaheuristic optimization methods," in *Proc. Int. Conf. Wind Energy Appl. Algeria (ICWEAA)*, Algiers, Algeria, Nov. 2018, pp. 1–6.

[37] M. Kharrich, M. Akherraz, and Y. Sayouti, "Optimal sizing and cost of a microgrid based in PV, WIND and BESS for a school of engineering," in *Proc. Int. Conf. Wireless Technol., Embedded Intell. Syst. (WITS)*, Apr. 2017, pp. 1–5.

[38] M. J. H. Moghaddam, A. Kalam, S. A. Nowdeh, A. Ahmadi, M. Babanezhad, and S. Saha, "Optimal sizing and energy management of stand-alone hybrid photovoltaic/wind system based on hydrogen storage considering LOEE and LOLE reliability indices using flower pollination algorithm," *Renew. Energy*, vol. 135, pp. 1412–1434, May 2019.

[39] M. M. Samy, S. Barakat, and H. S. Ramadan, "Techno-economic analysis for rustic electrification in Egypt using multi-source renewable energy based on PV/ wind/ FC," *Int. J. Hydrogen Energy*, vol. 45, no. 20, pp. 11471–11483, 2020, doi: 10.1016/j.ijhydene.2019.04.038.

[40] J. D. Vasanth, N. Kumarappan, R. Arulraj, and T. Vigneysh, "Minimization of operation cost of a microgrid using firefly algorithm," in *Proc. IEEE Int. Conf. Intell. Techn. Control, Optim. Signal Process. (INCOS)*, Mar. 2017, pp. 1–6, doi: 10.1109/ITCOSP.2017.8303149.

[41] K. S. Kavitha Kumari and R. S. R. Babu, "Effective microgrid cost reduction using dragon fly optimization algorithm and firefly algorithm," in *Proc. 5th Int. Conf. Comput., Commun. Secur. (ICCCS)*, Oct. 2020, pp. 1–5, doi: 10.1109/ICCCS49678.2020.9276979.

[42] M. Z. Rosselan and S. I. Sulaiman, "Dolphin echolocation algorithm for optimal sizing of grid-connected photovoltaic system," in *Proc. IEEE Int. Conf. Appl. Syst. Invention (ICASI)*, Apr. 2018, pp. 1252–1255, doi: 10.1109/ICASI.2018.8394518.

[43] M. Kharrich, O. H. Mohammed, S. Kamel, M. Aljohani, M. Akherraz, and M. I. Mosaad, "Optimal design of microgrid using chimp optimization algorithm," in *Proc. IEEE Int. Conf. Automat./XXIV Congr. Chilean Assoc. Autom. Control (ICA-ACCA)*, Mar. 2021, pp. 1–5, doi: 10.1109/ICAACCA51523.2021.9465336.

[44] R. Gupta, A. M. Gaur, and A. N. Mahajan, "Application of oppositional runner root algorithm (ORRA) for economic optimization of micro grid," in *Proc. Int. Conf. Adv. Electr., Comput., Commun. Sustain. Technol. (ICAECT)*, Feb. 2021, pp. 1–5, doi: 10.1109/ICAECT49130.2021.9392447.

[45] H. A. El-Sattar, H. M. Sultan, S. Kamel, A. S. Menesy, and C. Rahmann, "Optimal design of hybrid stand-alone microgrids using tunicate swarm algorithm," in *Proc. IEEE Int. Conf. Automat./XXIV Congr. Chilean Assoc. Autom. Control (ICA-ACCA)*, Mar. 2021, pp. 1–6, doi: 10.1109/ICAACCA51523.2021.9465283.

[46] A. A. Z. Diab, H. M. Sultan, I. S. Mohamed, O. N. Kuznetsov, and T. D. Do, "Application of different optimization algorithms for optimal sizing of PV/wind/diesel/battery storage stand-alone hybrid microgrid," *IEEE Access*, vol. 7, pp. 119223–119245, 2019.

[47] F. Nejabatkhah, Y. W. Li, and A. B. Nassif, "Optimal design and operation of a remote hybrid microgrid," *CPSS Trans. Power Electron. Appl.*, vol. 3, no. 1, pp. 3–13, Mar. 2018, doi: 10.24295/CPSSTPEA.2018.00001.

[48] G. Yu, Z. Meng, H. Ma, and L. Liu, "An adaptive marine predators algorithm for optimizing a hybrid PV/DG/battery system for a remote area in China," *Energy Rep.*, vol. 7, pp. 398–412, Nov. 2021, doi: 10.1016/j.egyr.2021.01.005.

[49] H. M. Sultan, O. N. Kuznetsov, A. S. Menesy, and S. Kamel, "Optimal configuration of a grid-connected hybrid PV/wind/hydro-pumped storage power system based on a novel optimization algorithm," in *Proc. Int. Youth Conf. Radio Electron., Electr. Power Eng. (REEPE)*, Mar. 2020, pp. 1–7, doi: 10.1109/REEPE49198.2020.9059189.

[50] K. S. El-Bidairi, H. D. Nguyen, S. D. G. Jayasinghe, T. S. Mahmoud, and I. Penesis, "A hybrid energy management and battery size optimization for standalone microgrids: A case study for Flinders Island, Australia," *Energy Convers. Manage.*, vol. 175, pp. 192–212, Nov. 2018, doi: 10.1016/j.enconman.2018.08.076.

[51] A. S. Omar, A.-A.-A. Mohamed, T. Senjyu, and A. M. Hemeida, "Multi-objective optimization of a stand-alone hybrid PV/wind/battery/diesel micro-grid," in *Proc. IEEE Conf. Power Electron. Renew. Energy (CPERE)*, Oct. 2019, pp. 391–396, doi: 10.1109/CPERE45374.2019.8980178.

[52] EBA. (2020). *AVERT, U.S. National Weighted Average CO_2 Marginal Emission Rate, Year 2019 Data*. U.S. Environmental Protection Agency, Washington, DC, USA. Accessed: May 22, 2021. [Online]. Available: https://www.epa.gov/energy/greenhouse-gases-equivalencies-calculator-calculations-and-references

[53] A. A. Heidari, S. Mirjalili, H. Faris, I. Aljarah, M. Mafarja, and H. Chen, "Harris hawks optimization: Algorithm and applications," *Future Gener. Comput. Syst.*, vol. 97, pp. 849–872, Aug. 2019, doi: 10.1016/j.future.2019.02.028.

[54] S. Mirjalili and A. Lewis, "The whale optimization algorithm," *Adv. Eng. Softw.*, vol. 95, pp. 51–67, Feb. 2016, doi: 10.1016/j.advengsoft.2016.01.008.

[55] J.-S. Chou and D.-N. Truong, "A novel metaheuristic optimizer inspired by behavior of jellyfish in ocean," *Appl. Math. Comput.*, vol. 389, Jan. 2021, Art. no. 125535, doi: 10.1016/j.amc.2020.125535.

[56] A. Faramarzi, M. Heidarinejad, B. Stephens, and S. Mirjalili, "Equilibrium optimizer: A novel optimization algorithm," *Knowl.-Based Syst.*, vol. 191, Mar. 2020, Art. no. 105190, doi: 10.1016/j.knosys.2019.105190.

[57] M. Ghasemi, I. F. Davoudkhani, E. Akbari, A. Rahimnejad, S. Ghavidel, and L. Li, "A novel and effective optimization algorithm for global optimization and its engineering applications: Turbulent flow of water-based optimization (TFWO)," *Eng. Appl. Artif. Intell.*, vol. 92, Jun. 2020, Art. no. 103666, doi: 10.1016/j.engappai.2020.103666.

[58] The European Commission's Science and Knowledge Service. (Oct. 15, 2019). *Photovoltaic Geographical Information System*. Accessed: Jul. 15, 2021. [Online]. Available: https://re.jrc.ec.europa.eu/pvg_tools/en/#HR

[59] S. Husain and N. A. Shrivastava, "Stand-alone hybrid renewable energy system: Optimization and sensitivity analysis," in *Proc. Int. Conf. Electr. Electron. Eng. (ICE3)*, Feb. 2020, pp. 717–722, doi: 10.1109/ICE348803.2020.9122956.

MAHMOUD E. SALLAM received the bachelor's and Diploma degrees in electrical engineering from Ain Shams University (ASU), Cairo, Egypt, in 2000 and 2018, respectively, where he is currently pursuing the master's degree in electrical engineering. His main research interest includes the application of metaheuristic optimization techniques in microgrid sizing and control.

MAHMOUD A. ATTIA received the B.Sc., M.Sc., and Ph.D. degrees in electrical engineering from Ain Shams University (ASU), Egypt, in 2005, 2010, and 2015, respectively. He was a member of the Continuous Improvement and Quality Assurance Unit, Faculty of Engineering, ASU, until 2017. Since 2007, he has been a Teacher at ASU. He is currently working as an Associate Professor of electrical power engineering at Ain Shams University. He has authored many journal articles and conference papers. He is the author of the books *Optimal Allocation of FACTS Devices in Electrical Power Systems: A Genetic Algorithm Based Approach* (2013) and *Enhancing Power System Performance With Growing Wind Power Penetration: Optimal Allocation of FACTS* (LAP LAMBERT Academic Publishing, 2015). He contributed to the book *Sustainable Energy Technologies and Systems* (LAP LAMBERT Academic Publishing, 2019). His research interest includes the application of artificial intelligence, evolutionary, and heuristic optimization techniques to power system operation, planning, and control. He is a Reviewer of *Electric Power Components and Systems*, *Ain Shams Engineering Journal*, and *International Transactions on Electrical Energy Systems*. In 2009, he was on the Technical Committee of the ASU international conference ASCEE-3. He is an Editorial Member of *i-manager's Journal on Circuits and Systems* and the Editor-in-Chief of *i-manager's Journal on Instrumentation and Control Engineering*.

ALMOATAZ Y. ABDELAZIZ (Senior Member, IEEE) received the B.Sc. and M.Sc. degrees in electrical engineering from Ain Shams University, Cairo, Egypt, in 1985 and 1990, respectively, and the Ph.D. degree in electrical engineering according to the channel systems from Ain Shams University and Brunel University, U.K., in 1996. He has been a Professor of electrical power engineering with Ain Shams University, since 2007. He has authored or coauthored more than 450 refereed journals and conference papers, 35 book chapters, and six edited books with Elsevier, Springer, and CRC Press. In addition, he has supervised more than 80 master's and 35 Ph.D. theses. His research interests include applications of artificial intelligence and evolutionary and heuristic optimization techniques to power system planning, operation, and control. He is a member of the Egyptian Sub-Committees of IEC and CIGRE. He has been awarded many prizes for distinct research and international publishing from Ain Shams University and Future University in Egypt. He is the Chair of the IEEE Education Society Chapter, Egypt. He is an Editor of *Electric Power Components and Systems*. He is an editorial board member, an editor, an associate editor, and an editorial advisory board member for many international journals.

MARIAM A. SAMEH received the B.Sc., M.Sc., and Ph.D. degree in electrical engineering from the Faculty of Engineering, Ain Shams University, Cairo, Egypt, in 2008, 2014, and 2020, respectively. Her Ph.D. thesis contributes to the optimization control of photovoltaics. She started working as a T.A. at the Faculty of Engineering, Future University in Egypt, Cairo, from 2008 to 2014. Then, she continued working at Future University in Egypt as a L.A., until March 2021. She is currently working as an Assistant Professor of electric power engineering at the Faculty of Engineering, Future University in Egypt. Her research interests include power systems control, distributed generation, renewable energy systems, photovoltaic control, and interfaces.

AHMED H. YAKOUT received the B.Sc. and M.Sc. degrees from the Department of Electrical Power and Machines, Faculty of Engineering, Ain Shams University, Cairo, Egypt, in 2000 and 2005, respectively, and the Ph.D. degree in electrical engineering from the University of Strathclyde, Glasgow, U.K., in 2010. He is currently an Associate Professor at the Faculty of Engineering, Ain Shams University. His main research interests include modern control techniques, renewable energy, and electrical power systems analysis, stability, and control.